Conducting polymer nanoparticles for voltage-controlled release of pharmacological chaperones

Hamidreza Enshaei,[1] Anna Puiggalí-Jou,[1,2,*] Núria Saperas[1,*] and Carlos Alemán[1,2,*]

[1] *Departament d'Enginyeria Química, EEBE, Universitat Politècnica de Catalunya, C/ Eduard Maristany 10-14, Ed. I2, 08019 Barcelona, Spain*

[2] *Barcelona Research Center for Multiscale Science and Engineering, EEBE, Universitat Politècnica de Catalunya, C/ Eduard Maristany 10-14, Ed. C, 08019 Barcelona, Spain*

[*] anna.puiggali@upc.edu, nuria.saperas@upc.edu and carlos.aleman@upc.edu

Abstract

Pharmacological chaperones (PCs) are low molecular weight chemical molecules used for patients for some rare diseases caused primarily by protein instability. Controlled and on-demand release of PCs through nanoparticles is an alternative for cases in which long treatments are needed and prolonged oral administration could have adverse effects. In this work, pyrimethamine (PYR), which is a potent PC consisting on a pyrimidine-2,4-diamine substituted at position 5 by a *p*-chlorophenyl group and at position 6 by an ethyl group, has been successfully loaded in electroresponsive poly(3,4-ethylenedioxythiophene) nanoparticles (PEDOT NPs). The PYR-loading capacity was of 11.4 ± 1.5 %, both loaded and unloaded PEDOT NPs exhibiting similar size (215 ± 3 and 203 ± 1 nm, respectively) and net surface charge (-26 ± 7 and -29 ± 6 mV, respectively). In the absence of electrical stimulus, the release of the PC from loaded NPs is very low (1.6% in 24 h and 18% in 80 days) in aqueous environments. Instead, electrical stimuli sustained for 30 min enhanced the release of PYR, which was of ~50% when the voltage was scanned from –0.5 V to 0.5 V (cyclic voltammetry) and of ~35% when a constant voltage of 1.0 V was applied (chronoamperometry).

Introduction

Pharmacological chaperones (PCs) are small molecular weight drugs that are used when the primary cause of a disease is the instability of a particular protein. The hallmark of PCs is their ability to bind and stabilize their target proteins. [1-6] Although the use of PCs is considered a potential therapeutic strategy for the treatment of conformational diseases (*i.e.* those caused by structurally abnormal proteins that cannot fold properly and achieve their native conformation), the administration of too high doses by oral or intravenous routes can be sometimes counterproductive due to the inhibition of the target protein.[7-9] In those cases, special dosing regimens must be envisaged to maximize their stabilizing activity and minimize their inhibitory activity. Within this context, encapsulation of PCs in scaffolds for local delivery may be needed to control the effective drug distribution, the therapeutic dosing and the adverse effects of systemic drug administration.

Controlled delivery of PCs can be proposed using two very different release models. The sustained release model (*i.e.* without on/off control), which was firstly introduced in the sixties,[10] is based on the delivery at a programmed rate for a prolonged period of time. This model, which is controlled by the encapsulating scaffold, presents some limitations since sustained release systems are not responsive enough to the dynamic behaviour of biological systems, changes in the surrounding environment (*i.e.* pH, temperature, ionic strength) causing undesired effects in their performance.[11,12] The second model is based on the utilization of novel materials and modern fabrication technologies for the preparation of robust drug-loaded systems for on-demand delivery by changing the environment through external stimuli.[13] The on-demand release model allows to regulate the delivery rate according to the patient needs, enabling non-uniform drug administration when it is beneficial.[14] Accordingly, the on-demand delivery model

seems very appropriated for controlling the effective PC distribution, the therapeutic dosing and the adverse effects of systemic administration.

Despite the potential clinical interest of PCs, the encapsulation and release of these small ligands in smart carriers have been scarcely investigated,[15-17] while their on-demand release using external stimuli (e.g. UV- and visible light, pH and electric voltage) remains completely unexplored. Pyrimethamine (PYR; Scheme 1) is a synthetic derivative of ethyl-pyrimidine with potent PC properties for GM2 gangliosidosis, which is a neurodegenerative disorder caused by a deficiency of lysosomal β- hexosaminidase (β-hex).[18-20] Thus, some mutants of this enzyme show decreased folding stability and cause adult-onset form of lysosomal storage diseases, while PYR stabilizes such mutants sufficiently to allow more β-hex to reach the lysosome. In addition, PYR, which is commercialized under the trade name Daraprim®, is an antiparasitic drug against infections caused by protozoan parasites (*e.g.* malaria and toxoplasmosis)[21-24] and is a potent pro-apoptotic inducer in cancer cells (*e.g.* in metastatic melanoma cells).[25-27]

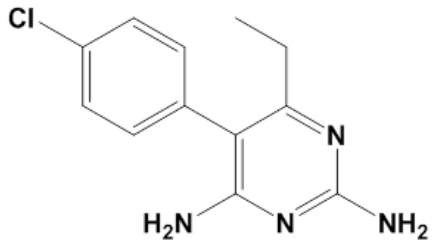

Scheme 1. Chemical structure of PYR

Despite their pharmacological interest, studies on the release of PYR from drug carriers are very scarce.[16,17,28] In an early study, Vandamme and Heller[16] prepared PYR-containing implants using bioerodible poly(ortho esters), releasing the drug by regulating the concentration of suberic acid. More recently, Lin and coworkers[28]

prepared PYR solid dispersions with different carriers to achieve release at gastric pH (~1-2). Finally, in a very recent work, Mollania and coworkers[17] prepared PYR-loaded carbon nanotubes (CNT/PYR), even though no controlled release was achieved in such study.

Conducting polymers are a special class of polymeric materials with conjugated structure, which exhibits both electronic and ionic conductivity through the mobility of electronic charge carriers (*i.e.* polarons and bipolarons) and ionic dopant agents, respectively. [29] Besides, the redox properties of conducting polymers are responsible for their intense electrochemical response. Due to their conducting and electrochemical properties, these materials have been used as carriers for on-demand drug release, which is controlled through externally applied voltage bias.[30] Among conducting polymers, poly(3,4-ethylenedioxythiophene) (PEDOT) has drawn the most attention due to its superior capacitive performance, high conductivity, stability in aqueous media and ambient conditions, and biocompatibility.[31-34] In recent years PEDOT nanoparticles (NPs) have been successfully used to encapsulate different types of anticarcinogenic and antimicrobial drugs (e.g. peptides and highly hydrophobic compounds).[35-37]

Herein, we describe for the first time the encapsulation and controlled release of a representative PC of therapeutic interest, PYR, in electro-responsive polymeric nanoparticles (NPs). It should be remarked that, in general, the encapsulation of drugs of small molecular size and bearing hydrophilic groups, such as the amino groups of PYR (Scheme 1), is challenging and problematic due to the rapid loss of drug to the external medium. For this study, PEDOT NPs have been used as carriers for the *in situ* encapsulation of PYR due to the capacity of this conducting polymer to interact with hydrophylic groups, hindering a fast release. After characterization of the loaded PEDOT NPs, hereafter named PEDOT/PYR NPs, the release of the drug by simple

diffusion (*i.e.* in the absence of external stimuli) and by imposing sustained electrostimulation was examined. Results showed that low release observed in the absence of stimuli can be significantly increased when the strength of PEDOT⋯PYR interactions is modulated by applying electrical stimuli through a potentiodynamic technique.

Results and discussion

PEDOT/PYR NPs and unloaded PEDOT NPs (control) were prepared through emulsion polymerization in a 12.5% methanol-containing aqueous medium. Methanol was used to solubilize PYR (8 mg/mL), which is poorly soluble in water. Ammonium persulfate (APS) was employed as oxidizing agent and dodecyl benzenesulfonic acid (DBSA) as both anionic surfactant (*i.e.* forming micelles) and dopant (*i.e.* stabilizing the formed PEDOT chains in their oxidized form). Due to the latter role, DBSA becomes a stable part of the NPs structure. The procedure used to prepare control PEDOT NPs was identical with the only exception that PYR was not incorporated into the methanol added to the aqueous monomer solution. A complete description of the synthetic procedure is provided in the Supplementary Material.

The FTIR spectra of free PYR, PEDOT/PYR NPs and PEDOT NPs are compared in Figure 1a. Free PYR exhibits broad and weak bands at 3443 and 3261 cm^{-1} (symmetrical and asymmetrical stretching of the $–NH_2$ group), a sharp and weak peak at 3073 cm^{-1} (C–H stretching from the aromatic ring), sharp and intense peaks between 1681 and 1409 (stretching vibrations of C=N and C=C from the aromatic rings), as well as at 1339 and 1243 cm^{-1} (C–H from CH_3 and C–N, respectively). On the other hand, PEDOT NPs show the characteristic FTIR peaks of PEDOT chains, which appear at 1648 and 1473 cm^{-1} (C=C stretching), 1351 cm^{-1} (C−C stretching), 1220 and 1061

cm^{-1} (C−O−C vibrations) and 842 cm^{-1} (stretch of the C−S bond in the thiophene ring). Also, weak but clearly defined bands attributed to DBSA dopant molecules were detected at 2923 and 2856 cm^{-1} (aliphatic $-CH_2$ and $-CH_3$ stretching), and 1693 cm^{-1} (C=C stretching from the phenyl ring). Finally, PEDOT/PYR NPs present mostly the bands associated with both PEDOT NPs and free PYR, as the–NH_2 group and the C=N stretching vibration.

Table 1. Atomic composition calculated from the XPS spectra for PEDOT and PEDOT/PYR NPs.

	C 1s	**N 1s**	**O 1s**	**S 2p**
PEDOT NPs	45.17	-	53.58	1.25
PEDOT/PYR NPs	67.89	0.56	30.34	1.21

Despite the successful identification of the loaded PC by FTIR, PEDOT/PYR NPs were complementarily studied by Raman spectroscopy and X-ray photoelectron spectroscopy (XPS). Unfortunately, the former technique was not conclusive since the spectrum of PEDOT/PYR NPs was dominated by the fingerprints of PEDOT NP (Figure S1), which was attributed to the strong absorbance of PEDOT chains. Although the interpretation of the obtained values is not simple due to the presence of DBSA as dopant agent, it is worth noting that N 1s is only detected for PEDOT/PYR NPs (Table 1 and Figure S2), supporting the successful loading of the PC. On the other hand, Figure 1b-c displays the high-resolution XPS spectrum in the N 1s region for PEDOT and PEDOT/PYR NPs. The nitrogen peak appears at 399.9 eV for PEDOT/PYR, which has been attributed to N−H and C−N from PYR.

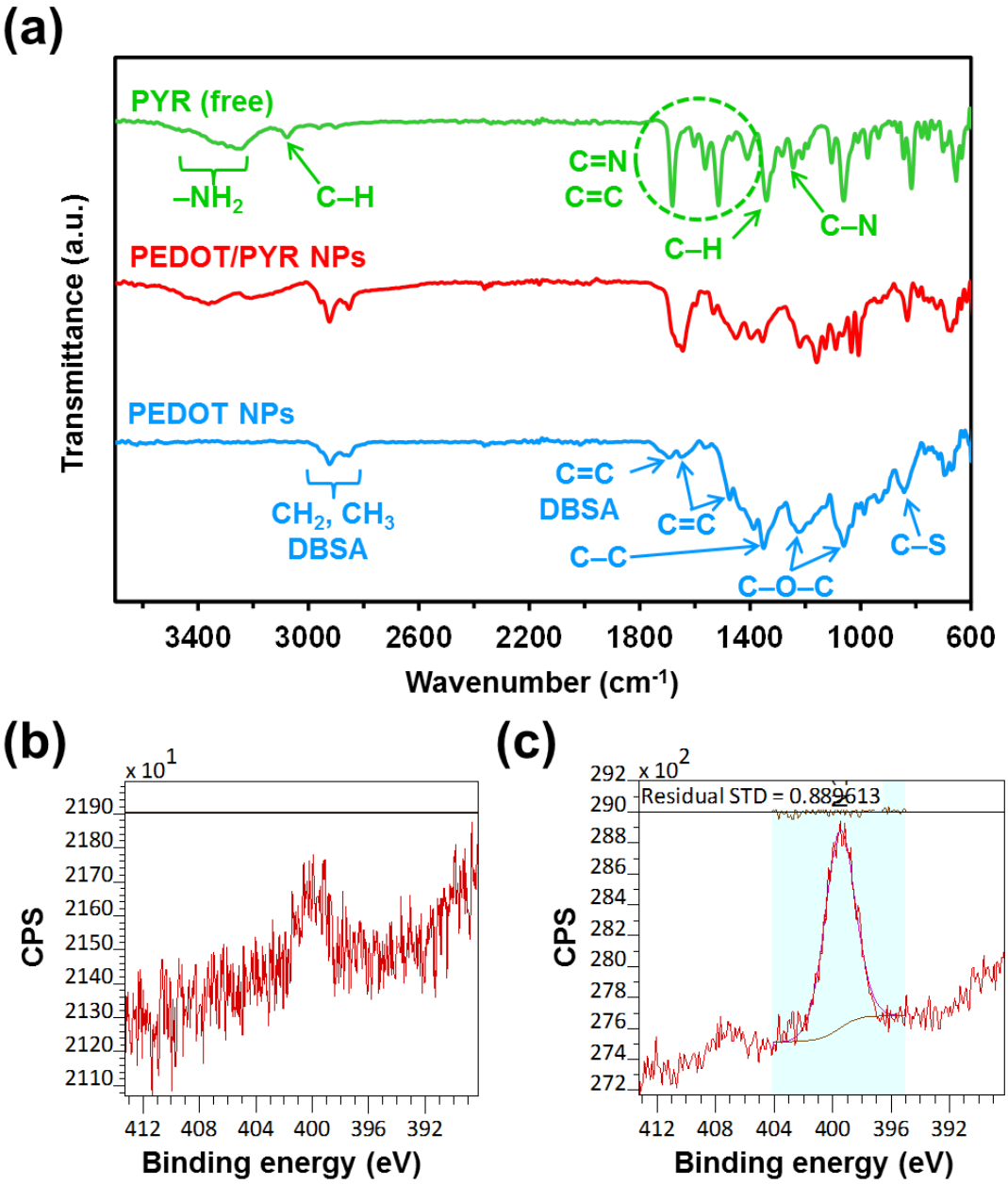

Figure 1. (a) FTIR spectra of free PYR, PEDOT/PYR NPs and PEDOT NPs. (b, c) High-resolution XPS spectra of the N 1s region for (b) PEDOT NPs and (c) PEDOT/PYR NPs.

Figure 2a displays the UV spectra of independent PEDOT/PYR samples in methanol, showing a specific absorption band at 280 nm. The PYR-loading capacity (LC, in %), which was expressed as the mass of loaded drug with respect to the total mass, was evaluated by using the absorbance at 280 nm and the calibration curve prepared by

dissolving the drug in methanol (Figure S3). Details are supplied in the Methods section (Supplementary Material). The PYR-LC was found to be 11.4 ± 1.5 %, this value being twice that reported for curcumin (CUR) encapsulated in PEDOT/CUR NPs by a similar procedure (CUR-LC = 5.9 ± 1.6 wt %).[37] Considering that CUR and PYR are both hydrophobic drugs of similar size (*i.e.* molecular mass: 368.38 and 248.71 g/mol, respectively), this difference has been attributed to the hydrogen bonding capacity of PYR, which exhibits two $–NH_2$ groups able to interact as donor groups with the oxygen atoms of the ethylenedioxy moiety of PEDOT chains. Figure 2b compares the UV spectra of free PYR, PEDOT NPs and PEDOT/PYR NPs, evidencing that the PC is not covalently attached to the polymers chains. Furthermore, the spectra do not reveal the formation of PYR···PEDOT π-π stacking interactions, supporting the fact that the two species mainly interact through hydrogen bonding.

The average diameter of PEDOT and PEDOT/PYR NPs, as obtained from dynamic light scattering (DLS) measurements was 215 ± 3 and 203 ± 1 nm, respectively (Figure 2c). The similarity in the size of the two types of NPs suggests that the PC is homogeneously dispersed in the polymeric matrix. On the other hand, the zeta (ζ)-potential of drug-loaded nanocarriers is very important, giving information on the charge at the surface of the particles and the tendency of the NPs to aggregate or to remain discrete. According to the DLVO electrostatic theory, the stability of a dispersion involving NPs with charged surfaces depends on the balance between the attractive van der Waals forces (steric stabilization) and the electrical repulsion because of the net surface charge. In general a ζ-potential above 25 mV (positive or negative) indicates that the electrostatic repulsive forces exceed the attractive steric forces and the system is kept in a relatively stable dispersed state. The ζ-potential measured for PEDOT and PEDOT/PYR NPs was -26 ± 7 and -29 ± 6 mV, respectively (Figure 1c),

indicating that PYR does not reduce the stability of the polymeric NPs dispersion. Indeed, such ζ-potential values reflect that loaded PYR molecules do not shield the surface charge of PEDOT NPs.

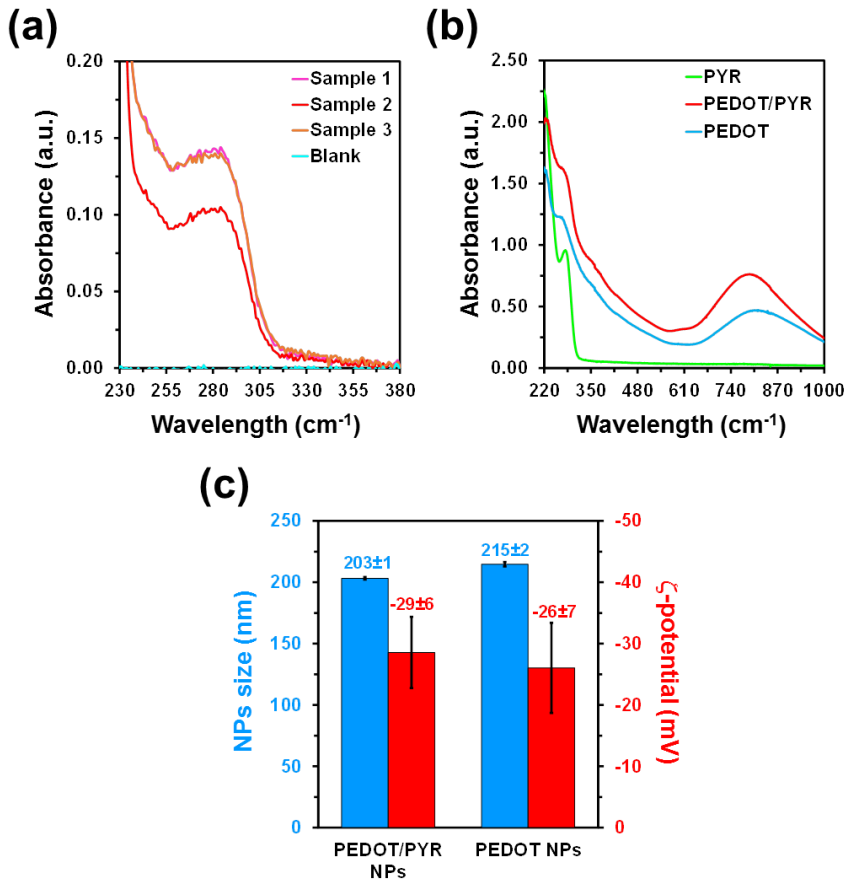

Figure 2. (a) UV-Vis spectra of PYR released from PEDOT/PYR in methanol (3 independent samples) compared to the blank. (b) UV-Vis spectra of free PYR, PEDOT/PYR NPs and PEDOT NPs. (c) Size (as determined by DLS) and ζ-potential of PEDOT/PYR and PEDOT NPs.

Representative high magnification (100k×) scanning electron microscopy (SEM) micrographs of PEDOT/PYR and PEDOT NPs are compared in Figure 3, while additional low magnification (50k×) micrographs are provided in Figure S4. In both cases NPs are relatively homogeneous in shape and size. PEDOT/PYR forms well defined spherical NPs with average diameter of 94 ± 12 nm, whereas unloaded PEDOT NPs exhibit an irregular shape with an average size of 109 ± 11 nm.

The sizes of the NPs visualized by SEM are approximately half of those registered by DLS. This has been attributed to two different features: 1) SEM measurements were performed in the dry state whereas DLS was measured in the solution state. Thus, the latter method provides the hydrodynamic diameter, which includes solvent molecules attached or adsorbed on the surface, while the former measures naked NPs; and 2) SEM is a number based NP size measurement that exhibits stronger emphasis on the smallest components in the size distribution whereas DLS is an intensity based measurement and emphasize on the larger NP size (*i.e.* intensity is proportional to r^6).

On the other hand, it was reported that shape and size of PEDOT NPs prepared by emulsion polymerization are affected by the surfactant type and concentration, respectively, which define the characteristics of the formed micelles.[38] Although DBSA leads to well-defined spherical micelles in water,[37,38] the addition of 12.5% methanol seems to promote micelle fusion resulting in irregular particles formed by the aggregation of smaller spherical particles. The micelle fusion with the apparent aggregation of small PEDOT NPs is probably inhibited by PYR. Despite such fusion phenomenon, the size of PEDOT NPs is only slightly larger than the diameter of spherical PEDOT/PYR NPs, as is shown in Figure 3 by their size distributions. 3D topographic AFM images of PEDOT/PYR and PEDOT NPs, which are included in Figure 3, are fully consistent with SEM micrographs, confirming that PEDOT/PYR samples are mainly made up of individual spherical NPs while the PEDOT samples exhibit irregular shapes due to fusion of nanostructures.

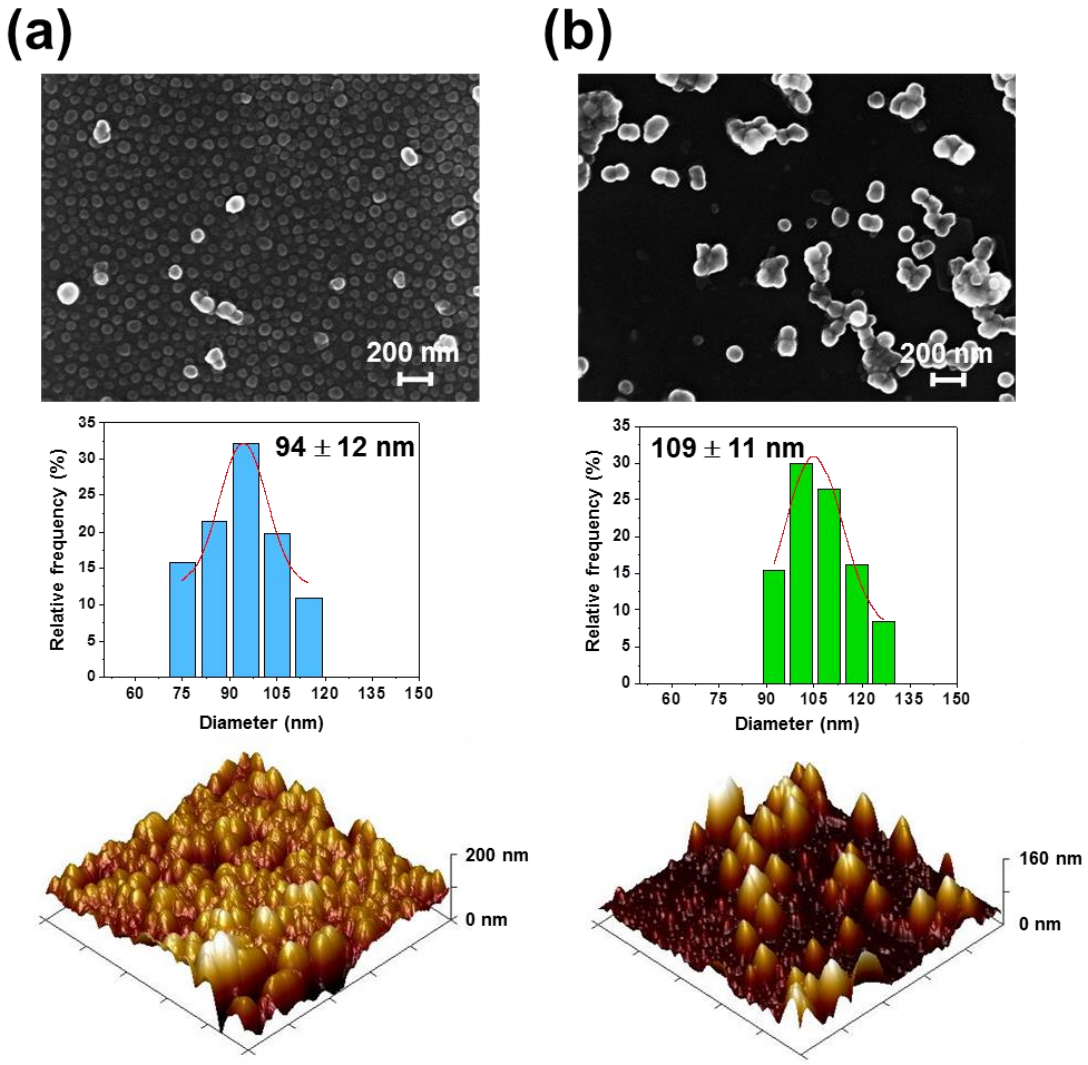

Figure 3. For (a) PEDOT/PYR NPs and (b) PEDOT NPs: SEM micrograph at 100kX magnification (top), diameter distribution histogram as determined from SEM images (middle), and 3D topographic AFM image (bottom) of 5 × 5 μm^2.

PEDOT/PYR NPs were incubated at 37 ºC in PBS (pH 7.4) and the *in vitro* release behaviour was studied over 80 days. The amount of released drug was evaluated by UV spectroscopy using the calibration curve obtained by plotting the absorbance measured at 280 nm against the PYR concentration. The cumulative release variation, which is represented in Figure 4a, exhibits a very slow evolution. The profile displays a biphasic regime consisting of an initial burst release for about 24 h, followed by a progressive but very slow release of PYR from PEDOT NPs. Thus, although about 1.6% of the PC

was released from PEDOT/PYR NPs within the first 24 h, a very slow release was evidenced thereon, reaching only 4.1% in 5 days (*i.e.* half of that expected from a sustained mechanism: 1.6% × 5 = 8.0%). Furthermore, the release achieved after 80 days was only around 18%. The initial burst release might be related to the free PYR adhered to the surface of PEDOT/NPs. The slow release observed after that have been attributed to the fact that the poor affinity of the encapsulated hydrophobic PC towards PBS does not compensate for the strength of the interactions between PYR molecules and oxidized PEDOT chains. Indeed, the solubility of PYR in water is very low (0.01 mg/mL),[39] evidencing that PYR···water interaction cannot compete with PYR···PYR and PYR···PEDOT interactions.

The solubility of PYR in ethanol (EtOH), almost 10 mg/mL, is three orders of magnitude higher than in water.[40] This property was used to obtain a complete and stable release profile as a function of the polarity of the release medium, which was achieved by replacing PBS by PBS:EtOH mixtures with increasing amount of co-solvent. More specifically, in such release assay, which took three weeks, the medium used for the first, second and third week was PBS, 90:10 PBS:EtOH, and 30:70 PBS:EtOH, respectively. The release profile is displayed in Figure 4b, while the profile obtained for each environment when a common starting point is imposed (*i.e.* release of 0% at the starting period of each environment) is depicted in the inset. The calibration curves obtained for such three media are plotted in Figure S5. Results show that, after one week, the release in PBS and 90:10 PBS:EtOH is 4.8% ± 0.5% and 3.4% ± 0.6%, respectively, indicating that the addition of a small amount of EtOH is not enough to facilitate drug diffusion from PEDOT NPs. Instead, the release is complete (100%) after 7 days of exposure when the 90:10 PBS:EtOH medium is replaced by 30:70 PBS:EtOH. These observations, which are consistent with the fact that PYR has much higher

affinity towards EtOH molecules than towards water molecules, allow us to conclude that PEDOT NPs can act as effective nanocarriers, minimizing the PC's loss by simple diffusion and, therefore, reducing undesired adverse effects and increasing PC bioavailability.

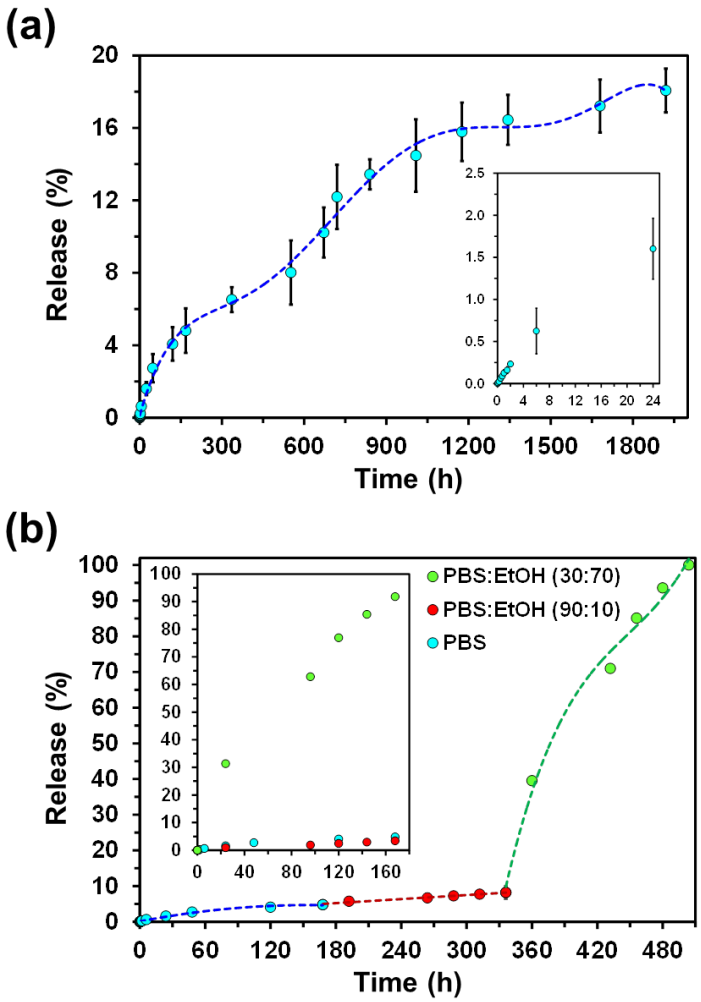

Figure 4. PC release from PEDOT/PYR NPs in: (a) PBS for 80 days at 37 ºC. Inset: magnification of the release profile for the first 24 h; and (b) PBS (first week), PBS:EtOH 90:10 (second week) and PBS:EtOH 30:70 (third week) at 37 °C. Inset: Drug release profiles from PEDOT/PYR NPs in PBS, PBS:EtOH 90:10 and PBS:EtOH 30:70 at 37 °C, which have been obtained by imposing a common starting point: release of 0% at the starting period (t= 0 h) in each environment.

In order to maximize the therapeutic efficacy of the PCs, an accurately controlled release should be achieved for prolonged and programmable treatments (*i.e.* extended

treatments based on time-controlled administration of drugs). Before examining the electrochemical response of PEDOT/PYR NPs, the redox behavior of PYR on a screen-printed carbon electrode (SPCE) was investigated by cyclic voltammetry (CV) using a phosphate buffered saline (PBS) solution at pH 7.4 as supporting electrolyte. The recorded voltammogram (Figure 5a) shows a well-defined anodic peak at 1.17 V in the anodic scan, even though no reduction peak appeared when the potential is reversed after oxidation. Although the characteristics of this voltammogram have been mainly associated to the irreversible electrochemical oxidation of the amino groups of PYR,[41] water electrolysis is also expected to contribute to the intensity and irreversibility of the peak.

Figure 5b compares the cyclic voltammograms obtained for bare and coated SPCEs, which were recorded in PBS at pH 7.4 and using a potential window comprised between –0.5 V (initial and final potential) and 1.4 V (reversal potential). The electrochemical activity of the bare SPCE increases noticeably upon coating with PEDOT or PEDOT/PYR NPs, as is reflected by the increment of area in the recorded voltammograms. Moreover, the enhanced electrochemical response of the coated SPCEs depends on the type of NPs, being much higher for PEDOT/PYR than for PEDOT. Considering that the amount of loaded PYR is not very high (PYR-LC = 11.4 ± 1.5 %), the large electrochemical response of PEDOT/PYR NPs in comparison to PEDOT NPs has been attributed to the synergistic effect of the two electroactive species, the PEDOT chains and the PC. Thus, the electroactivity of the PEDOT/PYR is significantly high in comparison to that of the two individual species (*i.e.* PEDOT NPs and free PYR), as shown in Figure S6. On the other hand, the electrochemical oxidation of PYR is still detected (as a shoulder) in the voltammogram recorded for the SPCE coated with PEDOT/PYR NPs.

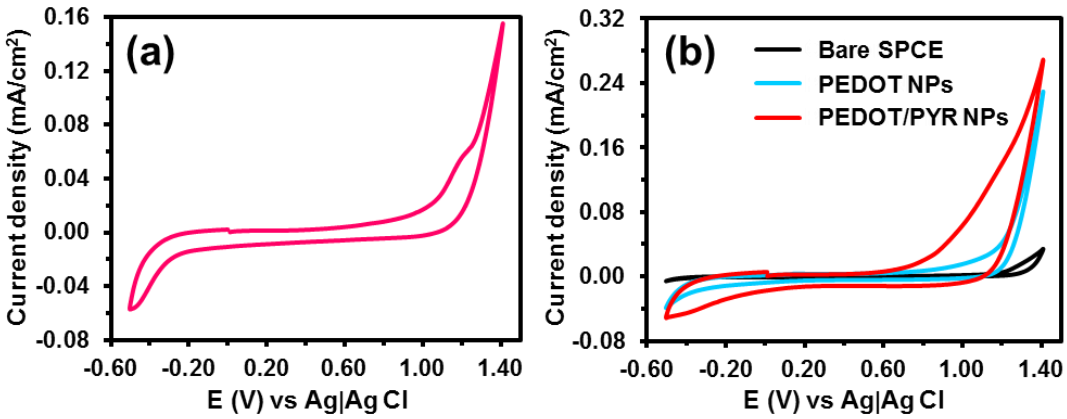

Figure 5. Cyclic voltammograms recorded from -0.5 to 1.4 V (scan rate: 100 mV/s) for (a) free PYR on SPCE and (b) bare (black) and coated (blue and red for PEDOT and PEDOT/PYR NPs) SPCEs.

The effect of the electrical voltage on the PYR release was examined using two approaches: 1) CV; and 2) chronoamperometry (CA). Electrostimulation by CV was performed by scanning the voltage in a window in which the chemical structure of the PYR could not be altered. Considering that PYR oxidizes at around 1.2 V, CV stimulation was applied by ramping the voltage linearly between –0.50 V (initial and final potential) to 0.50 V (reversal potential) at a scan rate of 100 mV/s (*i.e.* 10 s per CV cycle). CV stimulus was applied in a sustained way for 5, 15 and 30 min (*i.e.* 30, 90 and 180 consecutive CV cycles, respectively), the drug retention being evaluated after such periods of times. Figure 6a compares the shape of the voltammograms after 5, 10 and 15 min of sustained CV stimulation. It is worth noting that the shape and area of the voltammograms are similar, suggesting that the kinetics of the drug release is very slow. However, the reduction of the cathodic current density and the consequent enhancement of the tail close to the final potential indicate that the cathodic charge increases with time due to the release of the drug during the anodic scan. Thus, the release of PYR enhances the porosity of the NPs, favouring the exchange of ions at the interface with

the electrolyte and increasing the cathodic charge, as is reflected by the enhancement of the area in the cathodic scan. Figure 6b represents the amount of PYR released from PEDOT/PYR NPs after 5, 15 and 30 min of stimulation by CV, which is compared with that observed from control experiments conducting using the same intervals of time but without applying external stimuli. It is worth noting that, although the PYR release is very low in both cases, the amount of released drug determined by UV is ~50% higher for CV stimulated samples than for non-stimulated ones.

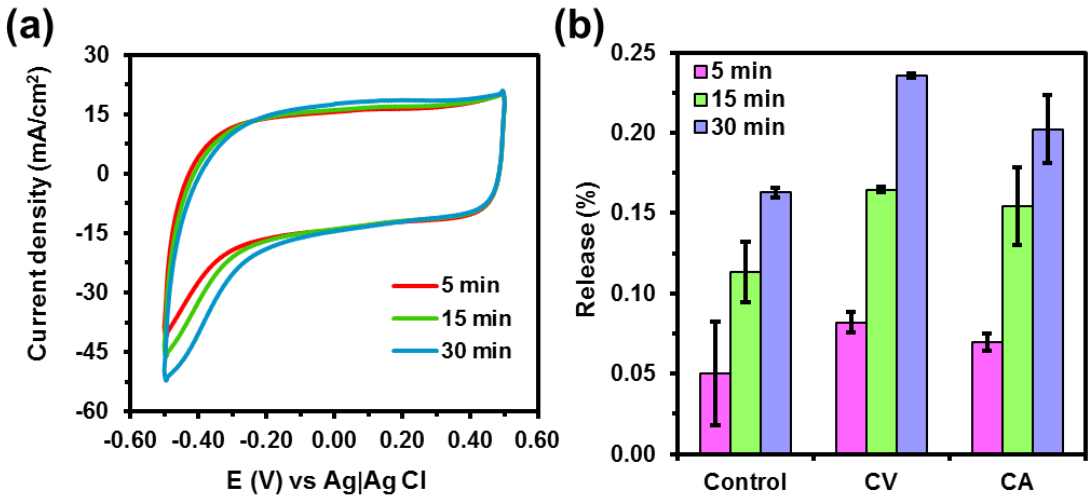

Figure 6. (a) Cyclic voltammograms recorded from –0.50 to 0.50 V (scan rate: 100 mV/s) for PEDOT/PYR NPs after 5, 15 and 30 min of CV stimulation. (b) PYR release during 5, 15 and 30 min without electrical stimulation (control) and with two different types of electrical stimulation CV (from –0.50 to 0.50 V at a scan rate of 100 mV/s) and CA (constant voltage of 1.00 V).

Electrostimulation was also examined by CA applying a constant voltage of 1.0 V during 5, 15 and 30 min. The amount of PYR released from loaded NPs at such time intervals is also plotted in Figure 6b. As can be seen, the drug released by CA stimulation is higher than that released in the absence of stimulus by ~35%. However, the comparison between CV and CA stimuli indicates that the former is more effective than the latter by ~15%. In both cases, the release mechanism is hypothesized to be

based on the effect of the voltage in the strength of PYR···PEDOT interactions. More specifically, after the injection of electrons, the amount of positive charge distributed along the oxidized PEDOT chains decreases and, therefore, $DBSA^-$ dopant anions are expelled from the polymeric NPs. This change in the oxidation level of the conducting polymer and the consequent reduction of $DBSA^-$ anions affects the strength of the interactions with the PC, which is partially released to the medium. This treatment is more effective when the variation of the voltage is performed using dynamic scans, which allows a continuous re-structuration of PYR in the polymeric NPs, than when a constant voltage is applied. On the other hand, the variation in the release was found to be larger for CA than for CV (Figure 6b). Thus, the application of a constant voltage of 1.0 V is expected to have more effect on the structure of PEDOT NPs (*i.e.* altering the structure of the NPs and reducing the control on the release) than the –0.50-to-0.50 V potential scan applied by CV.

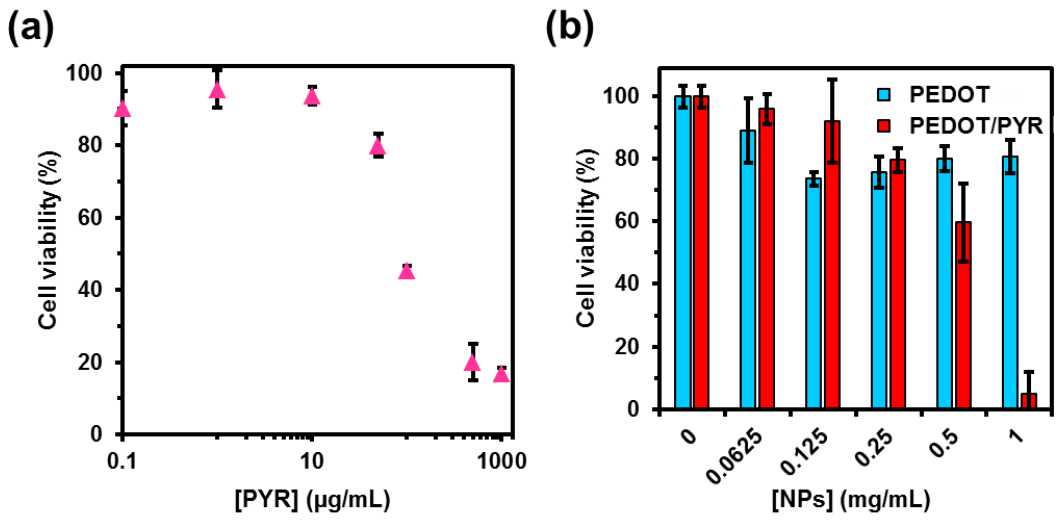

Figure 7. Dose-dependent viability of MG-63 cells treated with (a) free PYR and (b) PEDOT *vs* PEDOT/PYR NPs.

Finally, the cytotoxicity of PYR was assessed on the commercial human osteosarcoma MG-63 cell line. Figure 7a shows cell survival for the different

concentrations of such PC. The half-maximal inhibitory concentration (IC50) value of PYR was slightly lower than 100 µg/mL and, therefore, is classified as not cytotoxic. On the other hand, the cytotoxicity of PEDOT and PEDOT/PYR NPs was also examined using the MG-63 cell line. Figure 7b reflects that cells are tolerant to PEDOT NPs, exhibiting moderate reductions in cell viability. Instead, the cell viability decreases significantly when the concentration of PEDOT/PYR NPs is higher than 0.5 mg/mL are used. In any case, such IC50 value is still high, reflecting that the utilization of PEDOT/PYR NPs for sustained electrical stimulation is a safe strategy for the on-demand release of PC. The cytotoxic effect of DBSA, which was used dopant and stabilizer in the polymerization process, was studied in recent work.[35] Results showed that its cytotoxicity starts at low concentration, elimination by successive washing steps after the synthesis of the NPs being recommended.

Conclusions

One of the major advantages provided by PEDOT NPs is that the release of PYR is very low in absence of stimulus, increasing considerably (~50%) when sustained CV stimulation is applied for 30 min by scanning the voltage in a small window. Consequently, this approach holds great promise for regulating PYR to the desired optimal dosage. Other advantages that make PEDOT NPs beneficial for the controlled release of PCs are: 1) the simplicity of the synthesis, which allows the *in situ* PC-loading; 2) the high stability and fast response against electrical signals of the PC-loaded NPs, which are even higher than for unloaded NPs; and 3) the very low toxicity of PEDOT NPs. Recent studies have demonstrated that drug-loaded conducting polymer NPs can be injected *in vivo* and the drug-release be stimulated using microelectrodes.[42]

However, PEDOT NPs have the potential to be considered as promising electro-responsive nanocarriers for the on-demand wireless activated[43] delivery of other PCs.

Acknowledgements

This work was supported by Spanish and Romanian funding agencies. In Spain authors acknowledge MINECO/FEDER (RTI2018-098951-B-I00 and RTI2018-101827-B-I00) and the Agència de Gestió d'Ajuts Universitaris i de Recerca (2017SGR359 and 2017SGR373).

References

1. D. M. Pereira, P. Valentão and P. B. Andrade, *Chem. Sci.*, 2018, **9**, 1740–1752.
2. T. Mena-Barragan, A. Narita, D. Matias, G. Tiscornia, E. Nanba, K. Ohno, Y. Suzuki, K. Higaki, J. M. Garcia Fernandez and C. Ortiz Mellet, *Angew. Chem. Int. Ed. Engl.*, 2015, **54**, 11696–11700.
3. E. M. Sanchez-Fernandez, J. M. Garcia Fernandez and C. O. Mellet, *Chem. Commun.*, 2016, **52**, 5497–5515.
4. M. Convertino, J. Das and N. V. Dokholyan, *ACS Chem. Biol.*, 2016, **11**, 1471–1489.
5. M. H. Shin and H.-S. Lim, *Mol. Biosyst.*, 2017, **13**, 638–647.
6. Z. S. Hou, A. Ulloa-Aguirre and Y. X. Tao, *Expert Rev. Clin. Pharmacol.*, 2018, **11**, 611–624.
7. K. Bhattacharya, L. Weidenauer, T. Morán Luengo, E. C. Pieters, P. C. Echeverría, L. Bernasconi, D. Wider, Y. Sadian, M. B. Koopman, M. Villemin, C. Bauer, S. G. D. Rüdiger, M. Quadroni and D. Picard, *Nat. Commun.*, 2020, **11**, 5975.

8. V. Bernier, D. G. Bichet and M. Bouvier, *Curr. Opin. Pharmacol.*, 2004, **4**, 528–533.
9. L. Cortez and V. Sim, *Prion*, 2014, **8**, 197–202.
10. Y. Yun, B. K. Lee and K. Park, *Front. Chem. Sci. Eng.*, 2014, **8**, 276–279.
11. C. P. McCoy, C. Brady, J. F. Cowley, S. M. McGlinchey, N. McGoldrick, D. J. Kinnear, G. P. Andrews and D. S. Jones, *Expert Opin. Drug Deliv.*, 2010, **7**, 605–616.
12. S. Sershen and J. West, *Adv. Drug Deliv. Rev.*, 2002, **54**, 1225–1235.
13. B. P. Timko, T. Dvir, D. S. Kohane, *Adv. Mater.*, 2010, **22**, 4925–4943.
14. B.-B. C. Youan, *J. Control. Release*, 2004, **98**, 337–353.
15. E. Hamidreza, M. Brenda, L. J. del Valle, F. Estrany, C. Arnan, J. Puiggalí, N. Saperas and C. Alemán, *Macromol. Biosci.*, 2019, **19**, 1900130.
16. T. F. Vandamme and J. Heller, *J. Control. Release*, 1995, **36**, 209–213.
17. F. Mollania, N. L. Hadipour and N. Mollania, *J. Biotechnol.*, 2020, **308**, 40–55.
18. G. H. B. Maegawa, M. Tropak, J. Butner, T. Stockley, F. Kok, J. T. R. Clarke and D. J. Mahuran, *J. Biol. Chem.*, 2007, **282**, 9150–9161.
19. K. S. Bateman, M. M. Cherney D. Mahuran, M. B. Tropak and M. James, *J. Med. Chem.*, 2011, **54**, 1421–1429.
20. J. T. R. Clarke, D. J. Mahuran, S. Sathe, E. H. Kolodny, B. A. Rigat, J. A. Raiman and M. B. Tropak, *Mol. Genet. Metab.*, 2011, **102**, 6–12.
21. J. Friesen, S. Borrmann and K. Matuschewski, *Antimicrob. Agents Chemother.*, 2011, **55**, 2760–2767.
22. K. C. Okell, J. T. Griffin and C. Roper, *Sci. Rep.*, 2017, **7**, 7389.
23. A. Secreieru, I. C. C. Costa, P. M. O'Neill and M. L. S. Cristiano, *Molecules*, 2020, **25**, 1574.

24. R. R. Ben-Harari, E. Goodwin and J. Casoy, Adverse event profile of pyrimethamine-based therapy in toxoplasmosis: A systematic review, *Drugs R. D.*, 2017, **17**, 523–544.
25. M. Chen, I. Osman and S. J. Orlow, *Mol. Cancer Res.*, 2009, **7**, 703–12.
26. A. M. Giammarioli, A. Maselli, A. Casagrande, L. Gambardella, A. Gallina, M. Spada M, A. Giovannetti, E. Proietti, W. Malorni and M. Pierdominici, *Cancer Res.*, 2008, **68**, 5291–5300.
27. C. Tommasino, L. Gambardella, M. Buoncervello, R. J. Griffin, B. T. Golding, M. Alberton, D. Macchia, M. Spada, B. Cerbelli, G. d'Amati, W. Malorni, L. Gabriele and A. M. Giammariolo, *J. Exp. Clin. Cancer Res.*, 2016, **35**, 137.
28. P. Khatri, M. K. Shah, N. Patel, S. Jain, N. Vora and S. Lin, *J. Drug Deliv. Sci. Technol.*, 2018, **45**, 110–123.
29. T.-H. Le, Y. Kim and H. Yoon, *Polymers*, 2017, **9**, 150.
30. A. Puiggalí-Jou, L. J. del Valle and C. Alemán, *J. Control. Release*, 2019, **309**, 244–264.
31. M. J. Donahue, A. Sanchez-Sanchez, S. J. Qu and R. M. Owens, *Mater. Sci. Eng. R Reports*, 2020, **140**, 100546.
32. L. Groenendaal, G. Zotti, P. H. Aubert, S. M. Waybright and J. R. Reynolds, *Adv. Mater.*, 2003, **15**, 855–879.
33. D. Aradilla, F. Estrany and C. Alemán, *J. Phys. Chem. C*, 2011, **115**, 8430–8438.
34. G. Fabregat, B. Teixeira-Dias, L. J. del Valle, E. Armelin, F. Estrany and C. Alemán, *ACS Appl. Mater. Interfaces*, 2014, **6**, 11940–11954.
35. A. Puiggalí-Jou, L. J. del Valle and C. Alemán, *ACS Biomater. Sci. Eng.*, 2020, **6**, 2135–2145.

36. A. Puiggalí-Jou, S. Wedepohl, L. E. Theune, C. Alemán and M. Calderon, *Mater. Sci. Eng. C*, 2021, **119**, 111598.
37. A. Puiggalí-Jou, P. Micheletti, F. Estrany, L. J. del Valle and C. Alemán, *Adv. Healthc. Mater.*, 2017, **6**, 1700453.
38. N. Paradee and A. Sirivat, *Polym. Int.*, 2014, **63**, 106–113.
39. S. H. Yalkowsky, Y. He, P. Jain, Handbook of aqueous solubility data, Second Edition, CRC Press, Boca Raton, FL 2010, p. 877.
40. M. J. O'Neil (ed.), The Merck index - An encyclopedia of chemicals, drugs, and biologicals, Whitehouse Station, NJ: Merck and Co., Inc., 2006, p. 1374.
41. A.-E. Radi, H. M. Nassef and M. I. Attallah, *Anal. Methods*, 2015, **7**, 4159–4167.
42. N. Hosseini-Nassab, D. Samanta, Y. Abdolazimi, J. P. Annes and R. N. Zare, *Nanoscale*, 2017, **9**, 143–149.
43. H. Joo, Y. Lee, J. Kim, J.-S. Yoo, S. Yoo, S. Kim, A. K. Arya, S. Kim, S. H. Choi, N. Lu, S. Lee, S. Kim, S.-T. Le and D.-H. Kim, *Sci. Adv.*, 2021, **7**, eabd4639

Graphical abstract